

Magnetic properties and crystal structures of ordered perovskites

$\text{Sr}_2\text{TbRu}_{1-x}\text{Ir}_x\text{O}_6$

Yoshihiro Doi,^a Yukio Hinatsu,^a Ken-ichi Oikawa,^b Yutaka Shimojo^b and Yukio Morii^b

^aDivision of Chemistry, Graduate School of Science, Hokkaido University, Sapporo 060-0810, Japan

^bJapan Atomic Energy Research Institute, Tokai-mura, Ibaraki 319-1195, Japan

Received 25th January 2000, Accepted 11th April 2000

Published on the Web 21st June 2000

We have performed powder neutron diffraction measurements for $\text{Sr}_2\text{TbRuO}_6$ at 10 K and room temperature. It has been found that the crystal structure of this compound is a distorted perovskite ($a=5.7932(2)$ Å, $b=5.8107(1)$ Å, $c=8.2011(3)$ Å and $\beta=90.249(2)^\circ$) with the space group $P2_1/m$ (No.14) and a 1:1 ordered arrangement of Ru^{5+} and Tb^{3+} over the 6-coordinate B sites. Data collected at 10 K show that $\text{Sr}_2\text{TbRuO}_6$ has long range antiferromagnetic ordering involving both Ru^{5+} and Tb^{3+} . Each of these ions orders in a type I arrangement. The direction of the magnetic moments is canted by *ca.* 20° from the c axis. The magnetic susceptibility and specific heat measurements show the existence of magnetic transitions at 32 K and 41 K.

The magnetic properties of $\text{Sr}_2\text{TbRu}_{1-x}\text{Ir}_x\text{O}_6$ ($0 < x < 1$) are also reported in this paper. The structural data and the value of the effective magnetic moment indicate that these compounds adopt the valence configuration of $\text{Sr}_2\text{Tb}^{3+}(\text{Ru}_{1-x}\text{Ir}_x)^{5+}\text{O}_6$ ($x=0.0\text{--}0.7$) or $\text{Sr}_2\text{Tb}^{4+}(\text{Ru}_{1-x}\text{Ir}_x)^{4+}\text{O}_6$ ($x=0.85\text{--}1.0$). Evidence for the presence of a mixed valence state was not found. The magnetic transition temperature for $\text{Sr}_2\text{Tb}^{3+}(\text{Ru}_{1-x}\text{Ir}_x)^{5+}\text{O}_6$ decreases with increasing x . On the other hand, that for $\text{Sr}_2\text{Tb}^{4+}(\text{Ru}_{1-x}\text{Ir}_x)^{4+}\text{O}_6$ increases with x .

Introduction

In recent years, the solid-state chemistry of mixed-metal oxides containing platinum group metals has attracted a great deal of interest. These materials adopt a diverse range of structures and show a wide range of electronic properties. We have focused our attention on the structural chemistry and magnetic properties of ordered perovskite-type oxides $A_2\text{LnMO}_6$ ($A=\text{Sr, Ba}; \text{Ln}= \text{lanthanide element}; M=4\text{d or }5\text{d transition elements}$) in which the Ln and M ions often order; these compounds show a range of magnetic behavior at low temperatures.

Very recently, the perovskites $\text{Sr}_2\text{LnRuO}_6$ containing the Ln^{3+} and Ru^{5+} ions at the six-coordinate B sites have been investigated.^{1–5} These compounds have the ordered perovskite-type structure and become monoclinically distorted with increasing ionic Ln^{3+} radius. They showed an antiferromagnetic transition at 30–46 K and a complicated temperature-dependence of magnetic susceptibilities below the transition temperatures.¹ Powder neutron diffraction investigations indicated that Sr_2YRuO_6 and $\text{Sr}_2\text{LuRuO}_6$ are antiferromagnetic below 26 K and 30 K, respectively, and that the arrangement of the Ru^{5+} ions adopts a type I ordering.^{2,3} $\text{Sr}_2\text{ErRuO}_6$ and $\text{Sr}_2\text{HoRuO}_6$ show antiferromagnetic ordering at *ca.* 40 K and 36 K, respectively. This magnetic ordering involves both Ru^{5+} and Er^{3+} (or Ho^{3+}) and they order in a type I fashion.^{4,5} In these compounds, the magnetic interactions between Ru^{5+} ions are important, and the magnetic interactions between Ru^{5+} and Ln^{3+} also contribute to the antiferromagnetic ordering for magnetic Ln^{3+} ions. The variation in the magnetic behavior of these compounds should be mainly derived from the difference in the magnetic properties of Ln^{3+} ions. Therefore, it is important to study the magnetic properties of each compound in detail.

In this paper, we will study the crystal and magnetic structures and magnetic properties of $\text{Sr}_2\text{TbRuO}_6$ using powder neutron diffraction, magnetic susceptibility and specific heat measurements.

A series of ordered perovskites $\text{Sr}_2\text{LnIrO}_6$ ($\text{Ln}=\text{Ce, Sm-Lu}$)

have similar crystal structures to that of $\text{Sr}_2\text{LnRuO}_6$. Among them, $\text{Sr}_2\text{TbIrO}_6$ has an ordered arrangement between Tb^{4+} and Ir^{4+} ions and shows magnetic transitions at 27 K and 51 K.^{6,7} Therefore, it is interesting to synthesize solid solutions between $\text{Sr}_2\text{Tb}^{3+}\text{Ru}^{5+}\text{O}_6$ and $\text{Sr}_2\text{Tb}^{4+}\text{Ir}^{4+}\text{O}_6$, and to study the variation of the valence state of the B site ions with compositions and their magnetic properties. We will report also the crystal structures and magnetic properties of these $\text{Sr}_2\text{TbRu}_{1-x}\text{Ir}_x\text{O}_6$ solid solutions.

Experimental

Polycrystalline samples of $\text{Sr}_2\text{TbRu}_{1-x}\text{Ir}_x\text{O}_6$ ($x=0.0, 0.1, \dots, 0.8, 0.85, 0.9, 0.95$ and 1.0) were prepared by firing the appropriate amounts of SrCO_3 , Tb_2O_7 , RuO_2 and Ir (metal) first at 1173 K for 12 hours and then at 1473 K for 60 hours in air with intermediate regular grinding and pelletting. In addition, the specimens with $x=0.8\text{--}0.95$ were also prepared by heating up to 1573 K for 48 hours. The progress of the reactions was monitored by powder X-ray diffraction measurements.

Powder neutron diffraction profiles were measured at 10 K and room temperature for $\text{Sr}_2\text{TbRuO}_6$ using a high-resolution powder diffractometer (HRPD) in the JRR-3M reactor (Japan Atomic Energy Research Institute), with a Ge(331) monochromator ($\lambda=1.8230$ Å). The collimators used were 6°–20°–6°, which were placed before and after the monochromator, and between the sample and each detector. The set of 64 detectors and collimators, which were placed every 2.5 degrees, rotate around the sample. Crystal and magnetic structures were determined by the Rietveld technique, using the program RIETAN.⁸

The field dependence of the magnetization for $\text{Sr}_2\text{TbRuO}_6$ was measured at 10, 15, 20, 25, 38 and 100 K over the applied magnetic field range $-5 \text{ T} < H < 5 \text{ T}$, and the temperature dependence of the DC magnetic susceptibility was recorded in an applied field of 0.1 T over the temperature range 5–300 K, using a SQUID magnetometer (Quantum Design, MPMS5S).

DOI: 10.1039/b000689k

J. Mater. Chem., 2000, 10, 1731–1735 1731

The susceptibility measurements and the magnetization were performed under two sets of conditions, *i.e.*, after zero field cooling (ZFC) and after field cooling (FC).

Specific heat measurements for $\text{Sr}_2\text{TbRuO}_6$ were performed using a relaxation technique with a commercial heat capacity measuring system (Quantum Design, PPMS) in the temperature range 2–100 K. The sample in the form of a pellet was mounted on a thin alumina plate with apiezon (N grease) for better thermal contact.

Results and discussion

1. Crystal structure of $\text{Sr}_2\text{TbRu}_{1-x}\text{Ir}_x\text{O}_6$

Almost all the reaction products $\text{Sr}_2\text{TbRu}_{1-x}\text{Ir}_x\text{O}_6$ were finally formed in a single phase with a perovskite-type structure. However, some samples which have compositions of $x=0.8$ (prepared both at 1473 K and at 1573 K) and $x=0.85\text{--}0.90$ (prepared at 1473 K) were obtained as two kinds of perovskite phases. Their X-ray diffraction patterns were indexed on a monoclinic unit cell (space group $P2_1/n$), and their structural analyses using the Rietveld method show that the Ln and Ru/Ir ions are arranged in an alternating manner. The crystal structure of $\text{Sr}_2\text{TbRuO}_6$ is shown in Fig. 1.

Fig. 2 shows the variation of lattice parameters for $\text{Sr}_2\text{TbRu}_{1-x}\text{Ir}_x\text{O}_6$ with the x value. It is found that the lattice parameters for the compounds with $x=0.0\text{--}0.7$ are obviously larger than those for the compounds with $x=0.85\text{--}1.0$, and that the order of the magnitude of a and b is different between these two sets of compounds, *i.e.*, $a < b$ in the former compounds, and $a > b$ in the latter compounds. The average ionic radius of the B site ions is calculated to be *ca.* 0.74 Å for the case of Tb^{3+} and $\text{Ru}^{5+}/\text{Ir}^{5+}$, and it is *ca.* 0.69 Å for the case of Tb^{4+} and $\text{Ru}^{4+}/\text{Ir}^{4+}$. These results indicate that the compounds with $x=0.0\text{--}0.7$ have an ordered arrangement between Tb^{3+} and $\text{Ru}^{5+}/\text{Ir}^{5+}$ and those with $x=0.85\text{--}1.0$ have an ordered arrangement between Tb^{4+} and $\text{Ru}^{4+}/\text{Ir}^{4+}$ at B sites.^{1,6}

The diffraction pattern of a sample with $x=0.8$ which was prepared by heating at 1473 K for 60 hours shows the presence of two phases. They are $\text{Sr}_2\text{Tb}^{3+}(\text{Ru}_{1-x}\text{Ir}_x)^{5+}\text{O}_6$ and $\text{Sr}_2\text{Tb}^{4+}(\text{Ru}_{1-x}\text{Ir}_x)^{4+}\text{O}_6$. The ratio of these two phases could be estimated to be 59:41 from the Rietveld analysis. Heating at higher temperatures increases the ratio of the formation of the $\text{Sr}_2\text{Tb}^{3+}(\text{Ru}_{1-x}\text{Ir}_x)^{5+}\text{O}_6$ phase (to more than 90%), but it could not be obtained as a single phase.

These results indicate that $\text{Sr}_2\text{TbRuO}_6$ and $\text{Sr}_2\text{TbIrO}_6$ do not

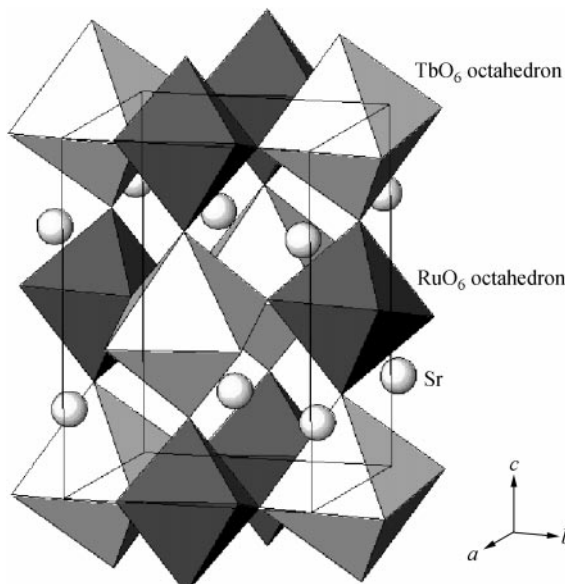


Fig. 1 The crystal structure of $\text{Sr}_2\text{TbRuO}_6$.

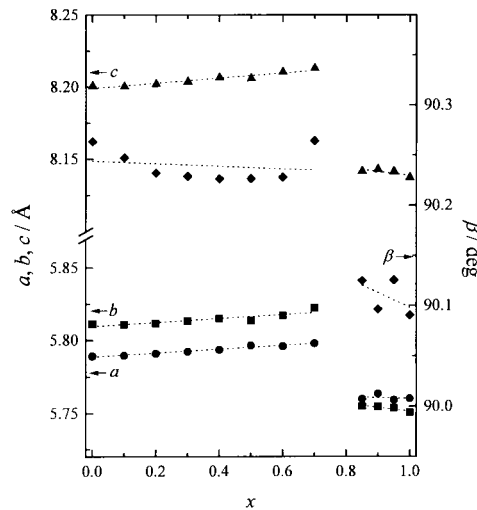


Fig. 2 Variation of lattice parameters for $\text{Sr}_2\text{TbRu}_{1-x}\text{Ir}_x\text{O}_6$ with x value.

form a complete solid solution. The borderline between these two phases is in the neighborhood of $x=0.8$ for $\text{Sr}_2\text{TbRu}_{1-x}\text{Ir}_x\text{O}_6$, but this x value may be shifted to some extent by the heating conditions.

For the later magnetic measurements, we used the samples with $x=0.0\text{--}0.7$, 1.0 (prepared by heating at 1473 K) and $x=0.8\text{--}0.95$ (prepared by heating at 1573 K).

2. Magnetic properties of $\text{Sr}_2\text{TbRuO}_6$ and $\text{Sr}_2\text{TbRu}_{1-x}\text{Ir}_x\text{O}_6$

The magnetic susceptibilities and specific heat capacities of $\text{Sr}_2\text{TbRuO}_6$ are plotted as a function of temperature in Fig. 3. The magnetic susceptibility data show that a magnetic transition occurs at 41 K, and a rapid increase of the magnetic moment (*ca.* 0.27 μ_{B}) is observed with decreasing temperature from 41 K to 32 K. The specific heat also shows a λ -type anomaly at 41 K. Magnetic hysteresis measurements at 38 K show the existence of a small hysteresis, and the remanent magnetization is estimated to be about 0.15 μ_{B} from the magnetic hysteresis curve. These results indicate that the magnetic transition observed at 41 K is an antiferromagnetic transition rather than a ferromagnetic one, and that the small remanent magnetization and the divergence between the FC and ZFC susceptibilities are derived from the weak ferromagnetic moment associated with this antiferromagnetism.

In addition, another broad peak may be observed at *ca.* 32 K in the specific heat vs. temperature curve. An anomaly of the magnetic susceptibility was also observed at *ca.* 31 K. However, the magnetic hysteresis curves measured around this tempera-

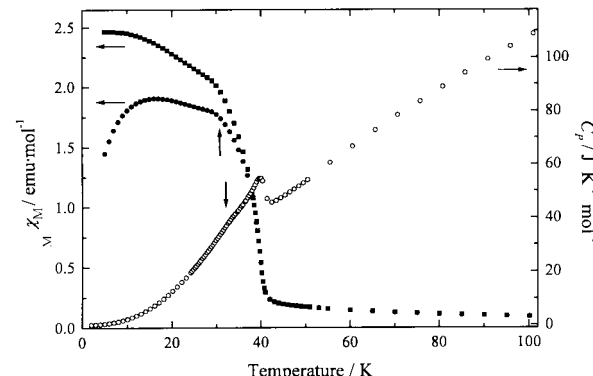


Fig. 3 Temperature dependence of the specific heat (\circ) and the ZFC (\bullet) and FC (\blacksquare) magnetic susceptibilities for $\text{Sr}_2\text{TbRuO}_6$. Two vertical arrows at 32 K and 31 K show specific heat and magnetic susceptibility anomalies, respectively (see text).

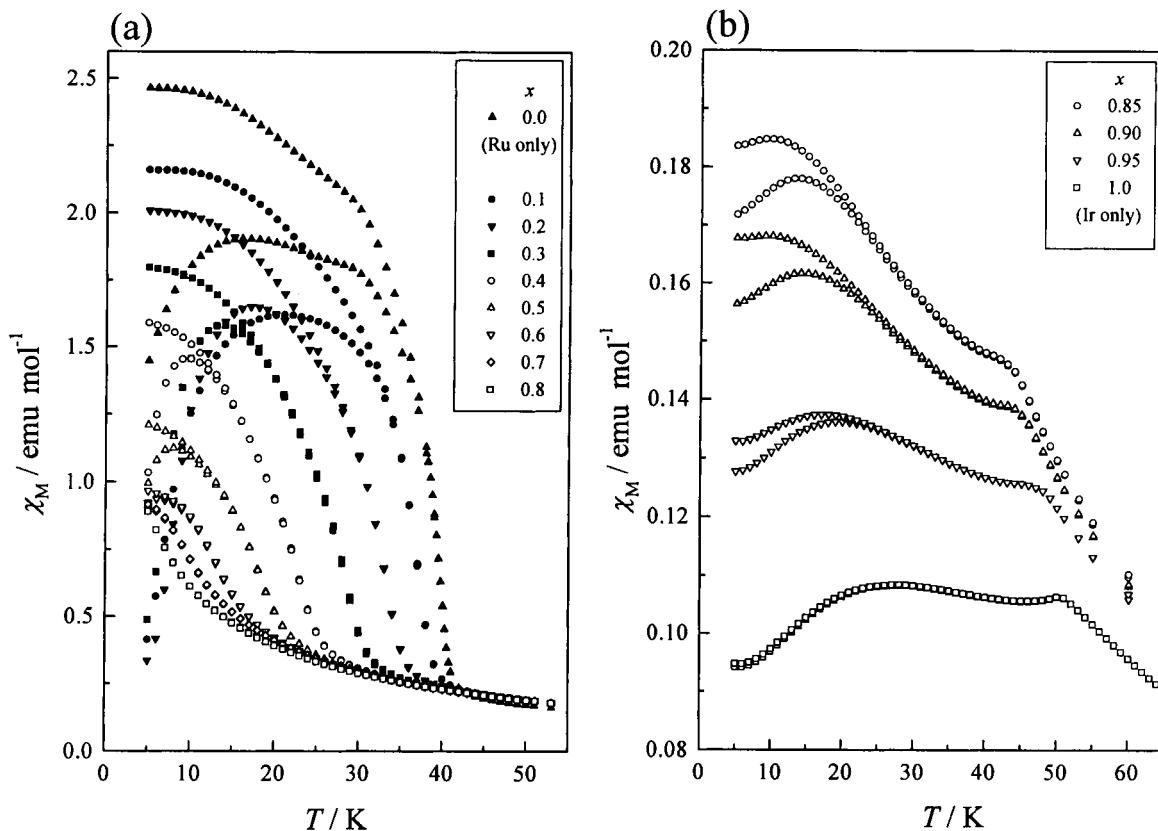


Fig. 4 Temperature dependence of the ZFC and FC magnetic susceptibilities for $\text{Sr}_2\text{TbRu}_{1-x}\text{Ir}_x\text{O}_6$: (a) $x=0.0\text{--}0.8$ and (b) $x=0.85\text{--}1.0$.

ture are very similar. This magnetic transition may be a reorientation of the magnetic moments.⁹

Fig. 4 shows the temperature dependence of the magnetic susceptibilities for $\text{Sr}_2\text{TbRu}_{1-x}\text{Ir}_x\text{O}_6$. The fitting of the Curie–Weiss law to the temperature dependence of magnetic susceptibilities at higher temperatures ($T > 100$ K) gives the effective magnetic moment (μ_{eff}) and Weiss constant (θ), which are plotted as a function of x value in Fig. 5. The effective magnetic moments are *ca.* $9.2 \mu_B$ for $x=0.0\text{--}0.7$ and *ca.* $8.0 \mu_B$ for $x=0.85\text{--}1.0$. This fact can be explained by the difference in the oxidation state of terbium ion in the solid solutions, *i.e.*, the terbium ion is in the trivalent state ($9.72 \mu_B$) in the former solid solutions and is in the tetravalent state ($7.94 \mu_B$) in the latter solid solutions. The results that the magnitudes of the magnetic susceptibilities for $\text{Sr}_2\text{Tb}^{3+}(\text{Ru}_{1-x}\text{Ir}_x)^{5+}\text{O}_6$ ($x=0.0\text{--}0.7$, Fig. 4(a)) are much larger than those for $\text{Sr}_2\text{Tb}^{4+}(\text{Ru}_{1-x}\text{Ir}_x)^{4+}\text{O}_6$ ($x=0.85\text{--}1.0$, Fig. 4(b)) can be explained by the same reason, that is, these results are consistent with the valence configuration in $\text{Sr}_2\text{TbRu}_{1-x}\text{Ir}_x\text{O}_6$ derived from the crystallographic data.

It is found that as the x value increases (*i.e.*, the proportion of Ir increases), the magnetic transition temperature of $\text{Sr}_2\text{Tb}^{3+}(\text{Ru}_{1-x}\text{Ir}_x)^{5+}\text{O}_6$ decreases (see Fig. 4(a)). Many experimental results indicate that the magnetic interactions between the Ir^{5+} ([Xe]4f¹⁴5d⁴ electronic structure) ions are weaker than those between the Ru^{5+} ([Kr]4d³) ions. For example, the ordered perovskites $\text{Sr}_2\text{Ln}^{3+}\text{Ru}^{5+}\text{O}_6$ ($\text{Ln}=\text{Eu-Lu}$) show magnetic transitions at low temperatures (30–46 K),¹ while the ordered perovskites $\text{Sr}_2\text{Ln}^{3+}\text{Ir}^{5+}\text{O}_6$ ($\text{Ln}=\text{Sm-Gd, Dy-Lu}$) do not show any magnetic transition down to 5 K.⁶ Hence, the decrease in the transition temperature with increase of the x value would be due to the decreasing proportion of the Ru^{5+} ions.

On the other hand, the magnetic transition temperature for $\text{Sr}_2\text{Tb}^{4+}(\text{Ru}_{1-x}\text{Ir}_x)^{4+}\text{O}_6$ ($x=0.85\text{--}1.0$, Fig. 4(b)) increases with the x value. This can be explained by taking account of the fact that the Ru^{4+} ion has a similar electronic configuration (4d⁴) to that for the Ir^{5+} (5d⁴) ion, *i.e.*, the magnetic exchange interaction between Ru^{4+} ions should be weak. The increase in the magnetic transition temperature with x is due to the increase in the proportion of Ir⁴⁺ ions (5d⁵) having strong interactions.

3. Neutron diffraction measurements for $\text{Sr}_2\text{TbRuO}_6$

It was ascertained, by X-ray diffraction measurements at room temperature, that $\text{Sr}_2\text{TbRuO}_6$ prepared in this study crystallized in a single phase.¹ In this study, we have performed neutron diffraction measurements both at room temperature and at 10 K. Rietveld analysis of the data collected at room temperature indicated that the crystal structure of $\text{Sr}_2\text{TbRuO}_6$ is a monoclinic perovskite with the space group $P2_1/n$ (No.14) and has an ordered arrangement between Tb^{3+} and Ru^{5+} ions over the six-coordinate B sites. The unit cell parameters are $a=5.7932(2)$ Å, $b=5.8107(1)$ Å, $c=8.2011(3)$ Å and $\beta=90.249(2)^\circ$ ($R_{\text{wp}}=6.26\%$, $R_I=1.96\%$, $R_F=1.39\%$ and $R_e=5.54\%$). This result is consistent with that of our previous X-ray diffraction measurements.¹ The observed and calculated

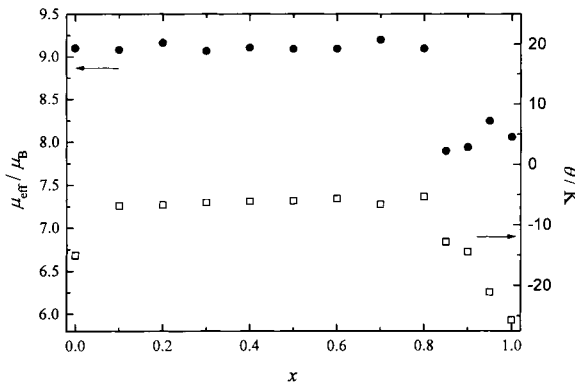


Fig. 5 Variation of the effective magnetic moment μ_{eff} (●) and Weiss constant θ (□) for $\text{Sr}_2\text{TbRu}_{1-x}\text{Ir}_x\text{O}_6$ with x value.

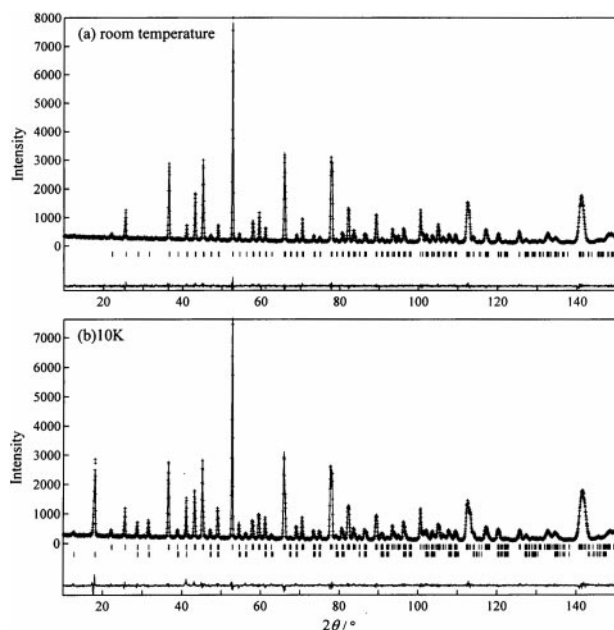


Fig. 6 Powder neutron diffraction profiles for $\text{Sr}_2\text{TbRuO}_6$ at room temperature (a) and at 10 K (b). The calculated and observed profiles are shown on the top solid line and cross markers, respectively. In (b) the nuclear reflection positions are shown as upper vertical marks and magnetic ones are shown as lower vertical marks. The lower trace is a plot of the difference between the calculated and observed intensities.

neutron diffraction profiles are shown in Fig. 6(a). The refined structural parameters, bond lengths and bond angles are listed in Tables 1 and 2, respectively.

Fig. 6(b) shows the neutron diffraction profile measured at 10 K. A number of low angle peaks, which are not observed at room temperature, appear in this profile. This fact indicates the presence of antiferromagnetic ordering. The positions of these magnetic reflection peaks very closely resemble those for $\text{Sr}_2\text{HoRuO}_6$ measured at 10 K,⁴ except for the difference in the intensity of the (001) peak ($2\theta \sim 12.8^\circ$). In the case of $\text{Sr}_2\text{HoRuO}_6$, this magnetic peak was negligibly weak, indicating that the alignment of the magnetic moments was parallel to the *c* direction. On the other hand, the corresponding (001) peak observed for the present $\text{Sr}_2\text{TbRuO}_6$ has significant intensity. We refined the magnetic structure of $\text{Sr}_2\text{TbRuO}_6$ using a model in which $\text{Sr}_2\text{TbRuO}_6$ has the same magnetic structure as $\text{Sr}_2\text{HoRuO}_6$ and the alignment of the magnetic

Table 2 Bond lengths (in Å) and bond angles (in degrees) for $\text{Sr}_2\text{TbRuO}_6$ at room temperature

Tb–O(1)	$2.215(5) \times 2$	Ru–O(1)	$1.966(5) \times 2$
Tb–O(2)	$2.225(5) \times 2$	Ru–O(2)	$1.964(5) \times 2$
Tb–O(3)	$2.232(5) \times 2$	Ru–O(3)	$1.958(5) \times 2$
Sr–O(1)	$2.565(8)$	2.796(7)	$2.913(7)$
Sr–O(2)	$2.542(8)$	2.813(8)	$2.880(8)$
Sr–O(3)	$2.552(7)$	2.688(6)	
O(1)–Tb–O(2)	$91.6(2)$	O(1)–Ru–O(2)	$90.4(3)$
O(1)–Tb–O(3)	$90.4(2)$	O(1)–Ru–O(3)	$90.4(3)$
O(2)–Tb–O(3)	$91.4(2)$	O(2)–Ru–O(3)	$90.0(2)$

moments cant from the *c* axis to some extent. We assume that all the magnetic moments are collinear.

Very good agreement between the observed data and calculated intensities was obtained. The refined structural parameters are listed in Table 1. The observed and calculated neutron diffraction profiles are shown in Fig. 6(b). The crystal structure at 10 K is similar to that at room temperature, and the monoclinic distortion is a little larger than that at room temperature. The magnetic structure of $\text{Sr}_2\text{TbRuO}_6$ is illustrated in Fig. 7. In this magnetic structure, the magnetic moments of both Tb^{3+} and Ru^{5+} ions are ordered anti-

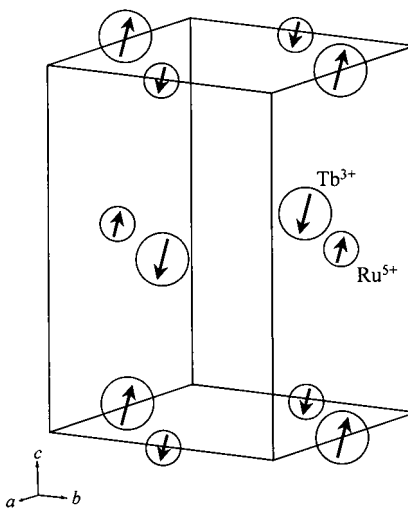


Fig. 7 The magnetic structure of $\text{Sr}_2\text{TbRuO}_6$. Diamagnetic ions are omitted. Larger circles Tb^{3+} ; smaller circles Ru^{5+} . The direction of the magnetic moments cant by about 20° against the *c* axis.

Table 1 Crystallographic data for $\text{Sr}_2\text{TbRuO}_6$ [space group $P2_1/n$ (No.14)] at 10 K and room temperature from the powder neutron diffraction profile

Atom	Site	<i>x</i>	<i>y</i>	<i>z</i>	<i>B</i> /Å ²	μ/μ_B
Room temperature ^a						
Sr	4e	0.0071(11)	0.0291(5)	0.2488(8)	0.8(1)	
Tb	2d	1/2	0	0	0.3(1)	
Ru	2c	1/2	0	1/2	0.3(1)	
O(1)	4e	0.2683(8)	0.2988(9)	0.0360(7)	0.5(1)	
O(2)	4e	0.1967(9)	-0.2301(9)	0.0387(6)	0.8(1)	
O(3)	4e	-0.0696(8)	0.4847(8)	0.2332(6)	0.9(1)	
10 K ^b						
Sr	4e	0.0058(10)	0.0330(5)	0.2494(7)	0.4(1)	
Tb	2d	1/2	0	0	0.2(1)	4.98(12)
Ru	2c	1/2	0	1/2	0.4(1)	2.99(11)
O(1)	4e	0.2697(8)	0.3027(9)	0.0374(7)	0.5(1)	
O(2)	4e	0.1939(8)	-0.2270(9)	0.0397(6)	0.2(1)	
O(3)	4e	-0.0714(8)	0.4824(8)	0.2319(6)	0.4(1)	

^a $a=5.7932(2)$ Å, $b=5.8107(1)$ Å, $c=8.2011(3)$ Å, $\beta=90.249(2)^\circ$, $R_{wp}=6.26\%$, $R_I=1.96\%$, $R_F=1.39\%$, $R_e=5.54\%$. ^b $a=5.7805(2)$ Å, $b=5.8072(1)$ Å, $c=8.1853(3)$ Å, $\beta=90.314(2)^\circ$, $R_{wp}=7.02\%$, $R_I=2.65\%$, $R_F=1.52\%$, $R_e=5.38\%$.

ferromagnetically. Each of these orders in a type I arrangement. The gradient of the magnetic moments against the *c* axis is about 20°, but the exact direction of them could not be determined. The ordered magnetic moments are 2.99(11) μ_B (for Ru⁵⁺) and 4.98(12) μ_B (for Tb³⁺). The ordered moment for Tb³⁺ is much smaller than the value of $g_J J$ (9 μ_B). This may be explained by the following reason. The magnetic moments of Tb³⁺ ions do not saturate at 10 K. This tendency has been experimentally found for Sr₂HoRuO₆ (6.68 μ_B at 10 K)⁴ and Sr₂ErRuO₆ (4.59 μ_B at 4.2 K).⁵

Acknowledgements

This work was supported by the Izumi Science and Technology Foundation.

References

- 1 Y. Doi and Y. Hinatsu, *J. Phys.: Condens. Matter*, 1999, **11**, 4813.
- 2 P. D. Battle and W. J. Macklin, *J. Solid State Chem.*, 1984, **52**, 138.
- 3 P. D. Battle and C. W. Jones, *J. Solid State Chem.*, 1989, **78**, 108.
- 4 Y. Doi, Y. Hinatsu, K. Oikawa, Y. Shimojo and Y. Morii, *J. Mater. Chem.*, 2000, **10**, 797.
- 5 P. D. Battle, C. W. Jones and F. Studer, *J. Solid State Chem.*, 1991, **90**, 302.
- 6 D. Harada, M. Wakeshima and Y. Hinatsu, *J. Solid State Chem.*, 1999, **145**, 356.
- 7 D. Harada, M. Wakeshima, Y. Hinatsu, K. Ohoyama and Y. Yamaguchi, *J. Phys.: Condens. Matter*, 2000, **12**, 3229.
- 8 F. Izumi, in *The Rietveld Method*, ed. R. A. Young, Oxford University Press, Oxford, 1993, ch. 13.
- 9 K. Tezuka, Y. Hinatsu, K. Oikawa, Y. Shimojo and Y. Morii, *J. Phys.: Condens. Matter*, 2000, **12**, 4151.